New Functional Bicomponent Fibers with Core/Sheath-Configuration Using Poly(phenylene sulfide) and Poly(ethylene terephthalate)

Stéphanie Houis*, Manfred Schmid, Jörn Lübben

Empa, Swiss Materials Science and Technology, Advanced Fibers, Lerchenfeldstrasse 5, CH-9014 St. Gallen, Switzerland

Received 19 April 2006; accepted 15 May 2007
DOI 10.1002/app.26846
Published online 17 July 2007 in Wiley InterScience (www.interscience.wiley.com).

ABSTRACT: Bicomponent fibers using the high-performance polymer poly(phenylene sulfide) (PPS) together with poly(ethylene terephthalate) (PET) were melt-spun. Both possibilities of using PPS, either as core or as sheath material, were realized to provide special functionalities like improved thermobonding capability, flame retardancy, or chemical resistance. Parameters that guarantee stable processing of PPS and PET during coaxial extrusion with different core/sheath volume ratios were explored. Microscopic studies of the cross-sections showed holes and cavities, which were formed at the interface between PPS and PET. Possible mechanisms for cavity formation were evaluated. Results of thermal and mechanical characterization by means of TGA, DSC, and tensile testing revealed a strong influence of the processing parameters, namely draw ratio and core/sheath volume ratio, on the crystallization and the tensile strength of the drawn fibers. By changing the core/sheath volume ratio from 2 to 0.5 in the PPS/PET fiber, the crystallinity of the PET-component was switched from 10 to 50%, whereas the crystallinity of the PPS dropped from 68 to 7%. It was determined that bicomponent fibers can exceed the strength of monocomponent fibers up to 28%. The flammability and chemical resistance of the new developed fibers were characterized. In contrary to what was expected, the encasing of PET with PPS reduced the flame retardancy, though PPS has a higher flame resistance than PET. The chemical resistance of the PET core against hydrolysis was imparted by coextruding a PPS sheath. © 2007 Wiley Periodicals, Inc. J Appl Polym Sci 106: 1757–1767, 2007

Key words: bicomponent fibers; poly(ethylene terephthalate); poly(phenylene sulfide); melt spinning; flame retardancy; chemical resistance

INTRODUCTION

Since the mid-1960s there has been a trend in the polymer industry to apply polymer blends and mixtures to modify material properties. In the synthetic fiber industry this trend is realized by manufacturing fibers, namely bicomponent fibers, consisting of two or more polymer components. Bicomponent fiber spinning can be defined as ''extruding two polymers from the same spinnerets with both polymers contained within the same fiber''.[1] Different types of bicomponent fibers can be produced: core/sheath, side-by-side, and matrix-fibril fibers.[2] Diverse functionalities can be imparted to these fibers in taking advantage of particular aesthetic, haptic, tactile, chemical or flame resistance properties, etc. in the sheath component and physical properties such as strength and conductivity in the core component.[3,4] Core/sheath bicomponent fibers are widely used as bonding fibers in the nonwoven industry. For this purpose the sheath of the fiber exhibits a lower melting point than the core.[5] At elevated temperature, the sheath melts creating bonding prints.[6,7] Although a vast amount of literature is available on various aspects of PET single component spinning,[8–12] there are only few reports on bicomponent spinning of PET with polypropylene (PP),[13] polyethylene (PE),[14] polystyrene (PS),[15] poly(butylene terephthalate) (PBT),[16] poly(butylene succinate/L-lactate) (PBSL) or poly(L-lactic acid) (PLLA).[3]

To our knowledge melt spinning and investigation of core/sheath bicomponent fibers consisting of PPS and PET has not been described in bicomponent fiber development so far. The thermal and crystallization behavior of unfilled and glass reinforced polyblends of PPS/PET as well as the isothermal crystallization of pure PET and PPS are well-studied.[17–21] During solidification complex interactions are expected of the two polymers in the spin-line. PPS exhibits a higher melting temperature ($\sim 280^\circ$C) than PET ($\sim 256^\circ$C). Therefore PPS would crystallize first in the presence of the supercooled melt of PET. This is due to a higher rate of crystallization for PPS in

**Present address*: Institut für Textiltechnik (ITA), RWTH Aachen, Eilfschornsteinstrasse 18, D-52062 Aachen, Germany.
Correspondence to: J. Lübben (joern.luebben@empa.ch).

Journal of Applied Polymer Science, Vol. 106, 1757–1767 (2007)

comparison to PET which is sluggish to crystallize.[17] Furthermore both nucleation and crystal growth of PET are accelerated by the solidified PPS.[18] In case of similar melting points and depending on the crystallizability of the individual component polymers, crystallization takes place concurrently or sequently. Depending on the position of the polymers in the bicomponent fiber, different crystallization kinetics are possible for the materials.

PPS is a high-performance thermoplastic polymer that combines thermal, mechanical, and chemical resistance as well as flame retardancy. Fundamental studies to the processability of PPS multifilaments were carried out by Carr and Ward.[22] It is known[8] that significant fiber structure development occurs during the spinning of bicomponent fibers, and that the structure and properties of the as-spun fibers depend on the thermal and stress history in the spinline. Because of the mutual interaction of the polymers in bicomponent spinning, the stress and thermal histories are completely different with respect to those in single-component spinning, especially when the two polymers differ significantly in their inherent properties such as elongational viscosity and solidification temperature.[23]

Fibers for technical and medical textiles or for bonded fiber fabrics require special functionalities like ''flame retardancy'' and ''chemical resistance''. Flame resistance is commonly measured by the highest Limiting Oxygen Index (LOI), the amount of oxygen needed to support combustion. However, the flammability of a given polymer depends upon both the physical state appearance of the product, as well as the particular fire scenario that is considered. Because of the difficult repeatability of this test, the number of fire tests in use is at least in the hundreds.[24] As the aim of this study is a pilot survey, a simple test, called basic burning test, was performed. This test can provide evidence of flammability considering the form and dimension of the filaments. Besides flammability test, also chemical resistance tests were carried out. In general PET is resistant to chemical attacks, but the ester linkage in the PET molecular chain can be attacked by some reagents such as acids or aqueous alkaline solution. Sodium hydroxide removes successive layers from the polymer fiber surface through chain scission and renders the surface more hydrophilic.[25] Therefore protection against hydrolysis might be an important issue. Using PPS with its chemical inertness against most chemicals as a protecting material can help to increase the life-time of PET-fibers under extreme environmental conditions.[26,27]

Possible applications of such new bicomponent fibers with PET in the sheath are self bonding fibers in nonwovens. Bicomponent fibers with PPS as sheath material are suitable for filter applications in drying processes. Filters with PET/PPS bicomponent fibers can be produced with less PPS and therefore with less material costs. Chemical protection against alkalis is needed in geosynthetics, which are expected to have a service life of up to 100 years.[27]

In this work spinning parameters are presented that guarantee both stable processing of filaments with core/sheath (c/s) configuration and sufficient quality of the as-spun yarn. The high-performance polymer PPS and the standard polymer PET were chosen for this study. The goal was to combine the positive properties of the two materials in one fiber by introducing the inherent functionalities of PPS ''flame retardancy'' and ''chemical resistance''. The resultant fibers were characterized regarding morphology, mechanical properties, crystallinity, decomposition, flammability and chemical resistance by means of optical microscopy (OM), scanning electron microscopy (SEM), tensile strength testing, differential scanning calorimetry (DSC), thermogravimetric analysis (TGA), a simple burning test, and treatment with alkaline solutions.

EXPERIMENTAL

Polymer materials and equipment

Pellets of PPS FORTRON 0320C0 with an average diameter of 3–5 mm were supplied by Ticona, Germany. Its physical properties are as follows: glass transition temperature (T_g) = 90°C, melting temperature (T_m) = 280°C, apparent melt viscosity at 310°C ca. 2000 Poise at an apparent shear rate of 2000 s^{-1}, and density ρ = 1.35 g/cm^3. Two types of PET were used. Type 1 (GL6105, Kuag Elana Oberbruch, Germany) is a bright fiber grade, crystallized chip with a nominal intrinsic viscosity of 0.62, T_g = 80°C, T_m = 259°C, and a density ρ = 1.33 g/cm^3. Type 2 (Clariant Huninque, France) is a transparent fiber grade chip with an intrinsic viscosity of 0.62, T_g around 80°C, T_m = 251°C, ρ = 1.33 g/cm^3. The polymers used for each bicompont fiber are indicated in Table I. All three polymers were dried at 120°C in vacuum for 12 h prior to extrusion.

Bicomponent fibers were produced on a pilot melt-spinning plant built by Fourné Polymertechnik (Alfter-Impekoven, Germany) to our specifications. The bicomponent plant enables the production of fibers consisting of two different polymers at laboratory scale with a throughput of up to several kilogram per hour. A schematic drawing of the melt-spinning plant is shown in Figure 1.

The polymers were melted using two extruders, one for the core component (1) and one for the sheath component (2), which were dosed by the spin

TABLE I
Produced Bicomponent Filaments, Production Parameters

Name of filament core/sheath (volume ratio)	DR	ST (°C)	VR spin pump V_{core}/V_{sheath}	RPM ratio spin pump U_{core}/U_{sheath}	MDV, v (m/min)	Count C_{exp} (dtex)	Diameter, D (μm)
PPS/PPS (1/1)	2	305	0.3/0.6	12/6	800	121.5	107.0
PPS/PPS (1/1)	3	305	0.3/0.6	12/6	1200	81	87.4
PPS/PPS (1/1)	3, 5	305	0.3/0.6	12/6	1400	69.4	80.9
[a]PET/PET (1/1)	2	260	0.3/0.6	12/6	800	121.5	107.0
[a]PET/PET (1/1)	3	260	0.3/0.6	12/6	1200	81	87.4
[a]PET/PET (1/1)	3, 5	260	0.3/0.6	12/6	1400	69.4	80.9
PPS/PET (1/2)	2	275	0.3/0.6	8/8	800	121.5	107.0
PPS/PET (1/2)	3	305	0.3/0.6	8/8	1200	81	87.4
PPS/PET (1/2)	4	260	0.3/0.6	8/8	1600	60.8	75.7
PPS/PET (2/1)	2	285	0.6/0.3	8/8	900	108	100.9
PPS/PET (2/1)	3	285	0.6/0.3	8/8	1350	72	82.4
PPS/PET (2/1)	4	285	0.6/0.3	8/8	1800	54	71.3
[a]PET/PPS (1/2)	2	300	0.3/0.6	9/9	800	136.7	113.5
[a]PET/PPS (1/2)	3	303	0.3/0.6	9/9	1200	91.1	92.7
[a]PET/PPS (1/2)	4	303	0.3/0.6	9/9	1600	68.3	80.3
[a]PET/PPS (2/1)	2	303	0.6/0.3	8/8	800	121.5	107.0
[a]PET/PPS (2/1)	3	303	0.6/0.3	8/8	1200	81	87.4
[a]PET/PPS (2/1)	3, 5	303	0.6/0.3	8/8	1400	69.4	80.9

[a] Filaments spun with PET of Type 1 (see: polymer materials and equipment).
DR, draw ratio; ST, spinneret temperature; VR, volume ratio; RPM, rotation per minute; MDV, maximal draw velocity.

pumps (3). The coaxially-combined polymer melt was extruded through a spinneret (4), featuring one hole for bicomponent-monofilaments with core/sheath-geometry. Monofilaments in the range of 50–100 dtex can be produced by this spinneret. Monomers and oligomers are sucked by a pump (5). The extrudate was melt-drawn after cooling down in the quenching chamber (6) with a quenching length of 1.4 m and a maximum air flow of 520 m^3/min. After cooling the filaments were drawn by three heated godets (9, 11, 13). The filaments were finally wound for storage and analysis by a winder (14). The melt-draw ratios were set between two and four times for the spun yarns.

Parameters like core/sheath ratio, draw ratio, and material combination were varied to survey the influence on the mechanical and structural behavior of the bicomponent fibers. Table I summarizes the different bicomponent fibers produced.

For conjugate spinning, the two polymer melts were brought together in the spinneret, which was kept between 260 and 305°C for all experiments. Exposure of PET to higher temperatures results in liquid melt flow; lower temperatures, in contrast, cause high viscose melt of the PPS component. For all bicomponent fibers the extruding core/sheath ratio was set to 1/2 (thick sheath) and 2/1 (thin sheath), respectively, under constant polymer mass flow. To get reference fibers with the same material in both core and sheath, PET/PET and PPS/PPS monocomponent fibers were melt-spun with an extruding ratio of 1/1.

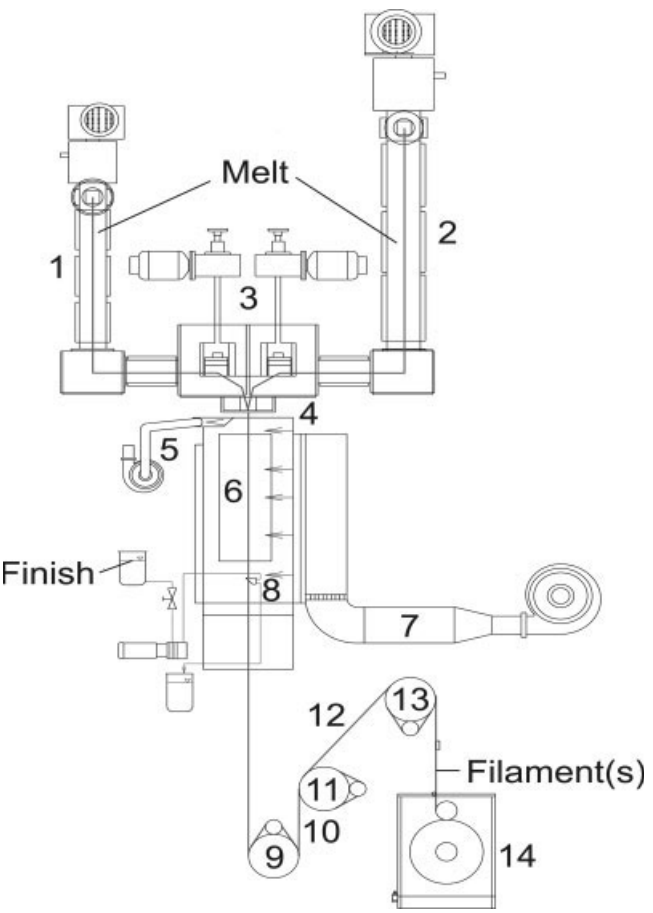

Figure 1 Schematic assembly of the bicomponent plant.

Instruments and procedures

Yarn count

The yarn count was measured according to DIN EN ISO 2060.[28] The final yarn count is calculated from the length and the mass of the sample using eq. (1):

$$C_{\text{test}} = \frac{m_c \times 10^3}{L} \quad (1)$$

where C_{test} stands for the count (dtex), m_c for the mass (g) and L for the length (m). The length used for the present study was 10 m.

The expected yarn count C_{exp} can also be calculated from the density ρ, the transported volume per rotation V/U and the number of rotations per minute U/t of the spin pump as well as from the winder take-up velocity v by using eq. (2):

$$C_{\text{exp}} = \frac{\rho(V/U)(U/t)}{v} \quad (2)$$

The yarn count is given in dtex and is defined as mass per 10,000 m length. The relationship between the Tex-system and the equivalent diameter of a round filament is given by eq. (3):

$$d(\mu\text{m}) = 20\sqrt{\frac{C\ (\text{dtex})}{\rho\ (g/cm^3)\pi}} \quad (3)$$

Humidity measurements

The humidity of the used pellets was measured on a AQUATRAC (Brabender Messtechnik KG, Germany) after drying. Remaining water in the pellets reacts with calcium hydride, generating hydrogen, which is measured and allows an exact determination of the water content. Fifty-six grams of polymer material was heated to 130°C. The accruing pressure was transformed and converted into a relative humidity value.

Tensile strength characterization

The tensile properties were characterized according to ISO 2062[29] on a STATIMAT M (TEXTECHNO Herbert Stein KG, Germany), with a gauge length of 250 mm and a strain rate of 250 mm/min. The pretensioning force was set to 0.5 cN/tex.

Thermal analysis

Thermogravimetric analysis (TGA) was carried out on a Mettler Toledo TA 4000 TG 50. The weight of all samples was kept between 15 and 30 mg. They were heated in an aluminum oxide pan without lid up to 750°C under 200 mL/min nitrogen and up to 850°C under oxygen. Differential scanning calorimetry (DSC) was performed according to DIN 53765[30] on a DSC 822e (Mettler–Toledo, Germany). The samples were heated from 25 to 350°C at 20 K/min for the first heating and at 10 K/min for the cooling and second heating. Crystallinity was estimated by means of eq. (4):

$$w_c = \frac{(\Delta H_{\text{melt}} + \Delta H_{\text{cc}} \times \text{mass portion}) \div \text{mass portion}}{\Delta H_{\text{literature}}} \times 100\% \quad (4)$$

where w_c is the crystallinity, ΔH_{melt} the measured heat of fusion, ΔH_{cc} the measured heat of fusion of the cold crystallization and $\Delta H_{\text{literature}}$ the heat of fusion of an ideal crystal. $\Delta H_{\text{literature}}$ of PET was taken to 164 J/g[31] and of PPS to 112 J/g.[32] As the bicomponent fibers consist of two materials, it is necessary to consider their weight proportion. The measured heat of fusion ΔH_{melt} was normalized by the weight portion of the respective fiber material, as both materials have almost the same density (ca. 1.35 g/cm^3).

Optical microscopy and Scanning Electron Microscopy

Optical microscopy images were obtained by a Laborlux 12 POL microscope (Leitz, Oberkochen, Germany) with a magnification of 250 for the cross sections and 100 for the examination after the tensile strength measurement with a pixel resolution of 1536 × 1152. Image processing (calibration, distances, determination of radius) was done with ImageAccess (Imagic Bildverarbeitung AG, Glattbrugg, Switzerland). Selected samples were examined with an 3200-C ECO-SEM (Amray, Bedford, MA, USA) in the ECO-mode at an accelerating voltage of 20 kV and a magnification of 400 for the examination of the surface after the chemical resistance tests. The samples were mounted on standard specimen stubs with silver paint and the stubs were then sputter-coated with gold.

Flammability and chemical resistance

Flammability was investigated using a so-called ''basic test''. For this measurement filaments were wound on a specimen holder with a constant feed of 50 mm/min. Afterwards the filaments were ignited at an angle of 45° for 15 s in the middle of the lower border with a flame of 20-mm length. Time until expiry of the flame was measured. Criteria to classify the flammability are the time until the flame

TABLE II
Classing for the Basic Flammability Test

Classing	Demand
Degree of flammability 3, highly combustible	Duration of burning 5–20 s
Degree of flammability 4, moderately combustible	Duration of burning > 20 s
Degree of flammability 5, low combustible	Flame does not reach upper border duration of burning < 20 s
Degree of flammability 6, noncombustible	No ignition, combustion or carbonise, need to proof noncombustibility

cone reaches the upper border or until the flame ceases to burn. The possible classifications under the ''basic test'' are given in Table II.[33]

For measuring the chemical resistance of the bicomponent fiber variations, both a 40% potassium hydroxide (KOH) solution and a 35% sodium hydroxide (NaOH) solution were prepared. Polyesters are generally readily attacked by alkalis. The hydrolysis of PET generates terephthalic acid and ethylene glycol in the final state. Complementary fibers (100 m) with thin PPS sheath (PET/PPS (2/1)) and thick PET sheath (PPS/PET (1/2)) were immersed in the alkaline solutions for 16 h, then washed with distilled water five times to remove the residues and thoroughly dried at standard conditions (T = 20°C, relative humidity = 65%) for 24 h. To judge the effect on the surface, SEM observation was carried out. Gravimetric changes were estimated by weighing the samples before and after chemical treatment under standard conditions.

RESULTS AND DISCUSSION

Yarn count and cross section

As a result of the constant polymer mass flow, comparable yarn counts were achieved (Fig. 2) for all bicomponent fibers.

The lower count for four-times-drawn PPS/PET (2/1) is justified by a higher take-up velocity of the first godet, the higher count of the PET/PPS (1/2) fibers by a higher spin pump rotation during production, as shown in Table I. All other samples have similar counts ranging from 117 ± 3 dtex for two-times drawn filaments to 56 ± 3 dtex for four-times drawn filaments.

At the interface between core and sheath cavities were detected. These holes appeared in all bicomponent fibers [Fig. 3(b,c)] and the PPS/PPS reference fibers [Fig. 3(a)], but not in the PET/PET reference fibers [Fig. 3(d)]. Such phenomena were not reported in literature so far.

Three possibilities for the occurrence of the cavities were considered: chemical reasons, procedural problems, and thermal behavior. Increased humidity in the raw materials after drying could lead to degradation. The handbook value for typical moisture contents after drying PPS and PET are 0.008% and 0.004%,[2,25] whereas the measured moisture content for PPS and PET was 0.005% and 0.022%, respectively. The high moisture content in the PET pellets would likely induce partial hydrolysis. It has been observed that only 0.01% H_2O in the PET chips can cause 10% decomposition in the melt.[2] Nevertheless, the occurrence of cavities because of remaining humidity of PET is unlikely, as no holes were observed in the PET/PET reference fibers. Humidity as a cause was also eliminated by trials with longer drying time for which cavities still occurred at the interface. Cavities were also found in the PPS/PPS reference fibers [Fig. 3(a)]. This implies that oligomers with a low melting point in the PPS pellets themselves could cause the problem. The oligomers vaporize at the processing temperature and form the observed cavities. This argument was also excluded, as such oligomers should volatilize during the drying process at temperatures around 120°C and the vacuum applied (<10 mbar). The microscopically visualized cross sections showed the cavity emerging always at the interface between core and sheath. Therefore the origin of the cavities is most likely caused by procedural problems, as probably induced by different viscosities and volume flow rates of the two different polymers.[26] As a consequence the two materials do not match rheologically. In our case, the core flows 3–6 times faster than the sheath, depending on the core/sheath volume ratio. This might lead to irregular flow conditions and the formation of cavities. As the used quenching chamber

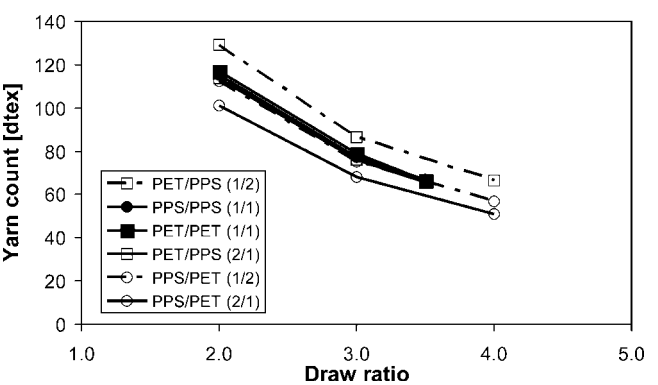

Figure 2 Yarn count of the produced filaments.

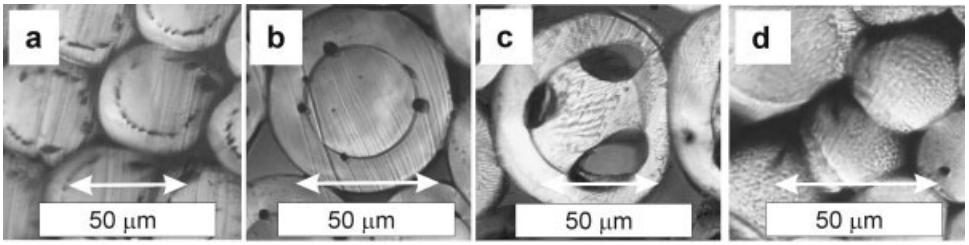

Figure 3 Cross section (a) PPS/PPS reference fiber; (b) PPS/PET (1/2); (c) PET/PPS (1/2); (d) PET/PET reference fiber.

was short (~ 1.5 m), a fast cooling had to be applied to reduce the temperature of the filaments sufficiently. This fact could have led to the development of the vacuoles: The material on the outside is already solidified while the center is still in a molten state. During congealing, shrinkage of the core material takes place that results in cavities. Regarding the linear thermal expansion coefficient across the flow direction, a ~ 1.8 times larger coefficient for PET (70×10^{-6} K^{-1}) in comparison with PPS (40×10^{-6} K^{-1}) was found.[34] Therefore holes should be larger for PET/PPS fibers than for PPS/PET, a tendency which turned out to be true [see Fig. 3(c)].

Composition and mass distribution

For a well-defined determination of the thermal behavior, the composition of the as-spun fibers was verified by TGA testing. Decomposition of the PPS/PPS and PET/PET reference fibers as well as the PPS/PET (1/2) and PET/PPS (1/2) bicomponent fibers is shown in Figure 4.

The first decomposition step starting at 394°C is attributed to PET, the second at 450°C to PPS as decomposition of PPS is initiated later. The PPS/PET (1/2) bicomponent fiber undergoes a significant decomposition in the first step because the fiber contains twice as much volume fraction of PET. The reverse trend can be observed for the PET/PPS (1/2) bicomponent fiber because half as much volume fraction of PET is comprised. The results for all bicomponents are summarized in Figure 5.

The masses were approximately distributed as expected, but the fibers possess a somehow larger content of PPS. This can be explained by the fact that the density was assumed to be constant for both components. In reality this is not the case. The smaller density of the PET in the molten state during the volumetric dosing with the spin pumps is assumed to be one reason for the smaller mass lost compared with PPS, according to eq. (2). A second reason is supposed to exist in a different mechanism of decomposition during the TGA heating process under nitrogen, which may lead to a relatively smaller mass lost of PET. This is the subject of further investigation.

Crystallinity and mechanical properties

We also investigated the structural state of the as-spun bicomponent fibers using DSC. Traces of a bicomponent fiber and the reference fibers are shown in Figure 6.

The melting peaks of PPS and PET can clearly be distinguished; the first peak refers to PET, the second to PPS. PPS melts at a higher temperature. Cold crystallization exotherms are present in all bicomponent fibers, an observation that is known for drawing single component fibers.[35,36] The presence of cold crystallization exotherms is attributable to the presence of a poorly oriented and uncrystallized PET or PPS component.

Figures 7 and 8 show the crystallinity derived from the DSC graphs as a function of draw ratio both for the PPS component and the PET component in the bicomponent fibers by means of eq. (4).

The crystal content rises with increasing draw ratio because of the molecular chain alignment. In case of the pure PPS and PET reference fibers similar crystal contents of 24–27% were found. In the bicomponent fiber systems only the material with a major content in the fiber showed a significant crystallinity. The sums of the crystallinities measured for the PPS/PET-systems (78% for PPS/PET (2/1), 57% for PPS/PET (1/2)) are higher than those measured for

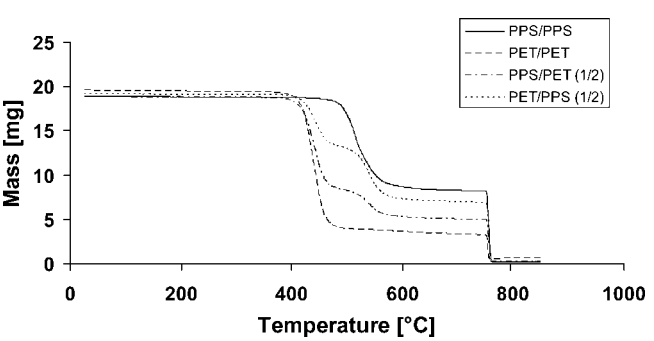

Figure 4 TGA graph of reference and bicomponent fibers.

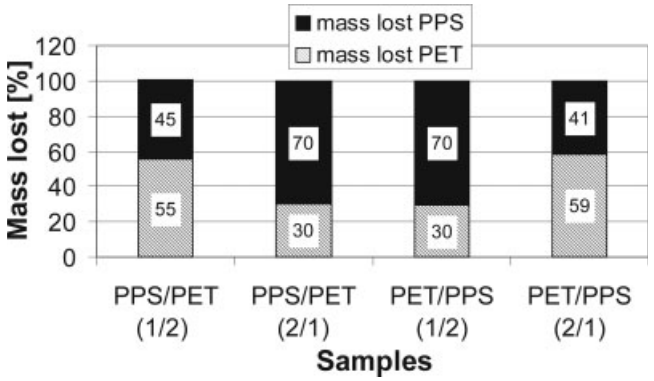

Figure 5 Mass lost for PPS and PET during TGA testing.

the PET/PPS-systems (42% for PET/PPS (1/2), 44% for PET/PPS (2/1)).

PPS exhibits a higher rate of crystallization, whereas PET is sluggish to crystallize. Thus, PPS would crystallize in the presence of a supercooled blend. Shingankuli et al.[37] showed in their studies on crystallization behavior of PPS/PET-blends that the presence of PET facilates the nucleation of PPS, whereas the PET crystallization rate increased owing to a heterogeneous nucleation provided by the PPS, which had already crystallized first. In the fiber system the polymers are barely mixed (see Fig. 3). Thus the interaction most likely takes place at the interface. The crystallization behavior is also affected by the heat transfer from the core to the interface sheath/air. Heat transfer seems to be responsible to a greater extent for the crystallization behavior of the polymers as indicated by the completely different crystallization behavior of PPS/PET (1/2) and PPS/PET (2/1).

PPS as sheath polymer crystallizes firstly owing to efficient cooling at the interface sheath/air. Efficient cooling of the PPS-sheath leads to faster crystallization, less time for orientation of the macromolecules in the quenching chamber and therefore to incomplete crystallinity of 17–21% (Fig. 7). It turned out that the crystallinity of the core polymer having a lower melting point, PET in our case, remains small due to stress relaxation, but crystallinity increases from 21% to 27% with increasing core/sheath vol-

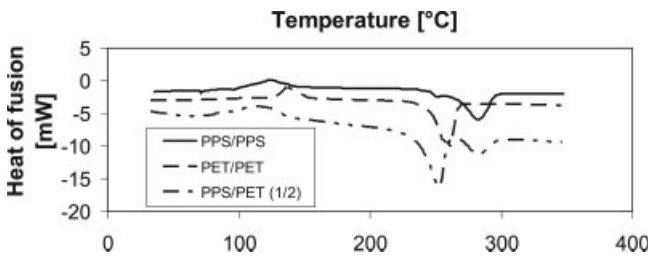

Figure 6 DSC traces for bicomponents and reference fibers.

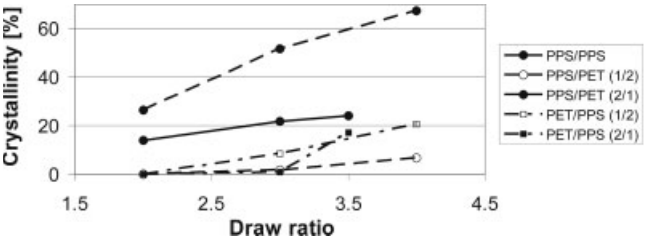

Figure 7 Crystal content of the PPS component.

ume ratio as demonstrated in Figure 8. Shingankuli et al. showed that the isothermal crystallization time for PPS at 240°C is about six times lower than that for PET at 200°C.[21] Blending PET with PPS accelerates the crystallization of PET significantly, but at 240°C the crystallization time for blended PET is more than 10 times higher than that for PPS.[21]

By placing PET as polymer with a lower melting point in the sheath, the degree of supercooling in the quenching chamber depends strongly on the heat transfer, the contact area at the PPS/PET interface, and the crystallization rate. The degree of supercooling required for PET crystallization in PPS/PET blends was shown[17] to be significantly lower compared to that required for pure PET. Two cases were observed in the PPS/PET systems: for a relatively thin sheath (PPS/PET (2/1)) the core polymer PPS solidified first as expected from the polymer crystallization kinetics.[20] For a relatively thick sheath (PPS/PET (1/2)) crystallization and solidification started most likely at the PET surface owing to a high temperature difference across the PET sheath from the surface to the PPS/PET interface. In that combination PPS remained the stress-relaxed unoriented part.

Considering the PPS component, bicomponent fibers with a thick PPS core (PPS/PET (2/1) showed the highest crystal content for this material. The crystallinity of PPS in this system is 2.8 higher than in the PPS/PPS (1/1) reference. This is an indication for interfacial interaction, as stated by El-Salmawy et al.[3,38] In their systems PET/PBSL and PET/PLLA the PET core showed a significantly higher crystallinity of 13–43% compared with that of a single PET fiber (6.3%), while the sheath polymer remained in

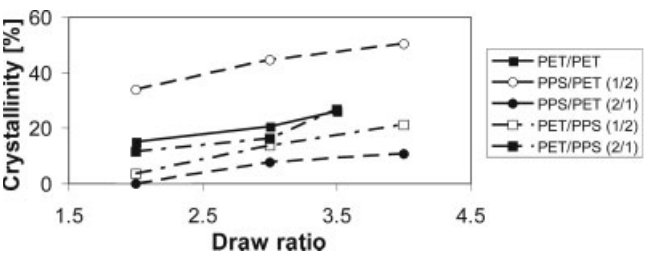

Figure 8 Crystal content of the PET component.

an amorphous state. They postulated that the driving force for this enhancement of crystallization depends on the interfacial shear arising between the two polymer layers. In our system the crystallization of PPS is most likely supported by the presence of PET. Jog et al.[19] mention two factors that could cause acceleration of the overall crystallization. Firstly, the supercooled melt of PET at the crystallization temperature of PPS (~ 230°C) possesses a higher crystal order than in the molten state at temperatures above the melting point of PET (~ 260°C). Secondly, PET and PPS exhibit similar chemical structures, which might cause a better match of the crystal structures at the interface PPS/PET. In view of the aromatic chain structure and polar linkages in both PPS and PET, greater secondary molecular interaction would be expected at the interface.[19]

The influence of varying volume flow ratio on crystallinity during high-speed melt spinning was studied by Radhakrishnan et al.[23] On a low-molecular-weight-PET/high-molecular-weight-PET (LMPET/HMPET) system, a strong influence on the occurrence of crystallization in the LMPET-core material was shown in changing the mass flow ratio from 1 : 1 to 1 : 4. Investigation of the Lorentz-density in the 1 : 1 combination indicates the occurrence of orientation-induced crystallization in LMPET. In the other case of the 1 : 4 combination, crystallization does not occur in LMPET as stress relaxation continues until the spinline cools down to glass transition temperature. This emphasizes the result described in our work, that only the major component in the PPS/PET system possesses a higher orientation and crystallinity.

In general, heat is retained longer in the sheath the thicker the layer is. Therefore higher orientation and crystallinity can occur owing to the faster movement of the macromolecular chains at higher temperatures. This fact explains the highest crystal content for the PET component in the system PPS/PET (1/2). Owing to the high spin head temperatures of 260–305°C (see Table I) the material kept a high temperature for a long time in the quenching chamber. Therefore the molecular chains had more time for orientation and crystallization. These assumptions are reflected in the tensile strength measurements (Fig. 9) where the system PPS/PET (1/2) possessed the highest tensile strength.

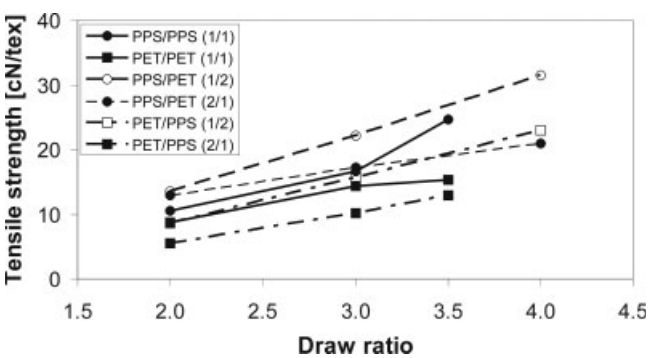

Figure 9 Maximum tensile strength of the bicomponent fibers.

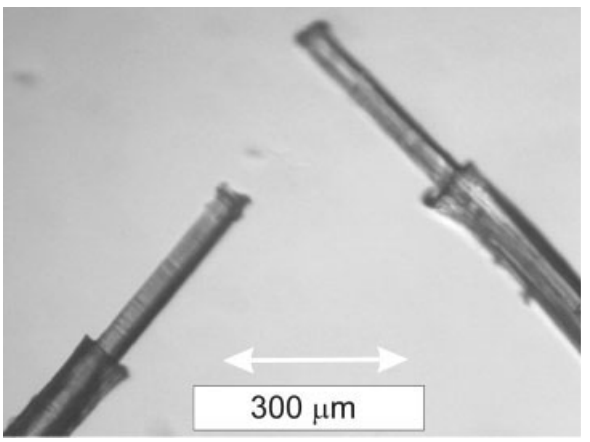

Figure 10 Pulled-out core on both end of the fracture of PET/PPS (1/2) bicomponent fibers.

Figure 9 shows the tensile strength of the produced fibers versus draw ratio. The observed increase in tensile strength with increasing draw ratio is a general tendency that can be related to increasing orientation and crystallization. Pure PPS unexpectedly showed a higher strength than pure PET. This may be contributed to partial hydrolysis of the PET fibers as a result of humidity in the pellets, resulting in decomposition of the molecular chains. This assumption is supported by the high standard deviation of ± 6.3 cN/tex of the PET fibers during tensile testing. A maximum strength of more than 30 cN/tex was observed for bicomponent fibers with a thin PPS core and a thick PET sheath. This fact can be accounted to high crystallinity (50.4%) and orientation of the PET component induced by increased heat supply as verified by DSC results (see Fig. 7 for PPS and Fig. 8 for PET). This fiber represents an example where a relatively crystalline sheath serves as mechanical strengthening whereas the core remains relatively amorphous.

The dimensions of the cavities certainly have also an influence on the tensile properties. Their sizes in the PPS/PET fibers were smaller than in the PET/PPS fibers which could additionally explain the higher tensile strength of the bicomponent fibers with PPS in the core. It appears that the thick PPS sheath of the PET/PPS (1/2) fiber provides higher strength compared with the PET/PPS (2/1) fiber, as the stress is distributed on the whole profile more evenly.

Furthermore, the core material defines the final strength when the sheath material crystallized first

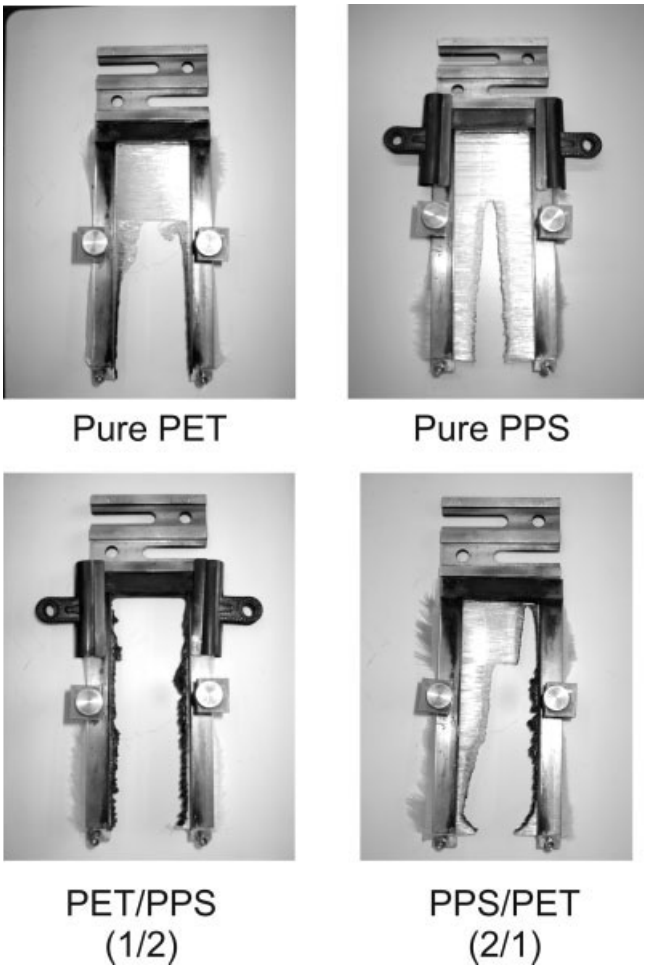

Figure 11 Wound fibers after flammability test.

(see Fig. 10). In the example shown (PPS/PET (1/2)) the semi-crystalline PET sheath broke first and the amorphous PPS core was pulled out in consequence. This two-step breaking behavior is the subject of further investigation.

Burning behavior

The different filaments were wound on a specimen holder and ignited for 15 s. The samples after the flammability test can be seen in Figure 11.

As expected the pure PPS reference fibers did not ignite but melted in vertical direction. According to the classification described in Table II the PPS fibers belong to Class V (low combustible) or even Class VI (noncombustible). This basis test is not suitable for demonstrating noncombustibility, therefore an additional test (electrical furnace test, DIN 4102) is necessary to prove noncombustibility.[33] The pure PET reference fibers inflamed and dripped as expected. The PET fibers are assigned to Class IV and are moderately combustible. The bicomponent fibers with PET in the sheath burned longer than the pure PET and also dripped. This bad fire performance could be due to the supporting PPS core: The PPS core could raise up the temperature even more and therefore contributes to the combustion of the PET component. Bicomponent fibers with PPS in the sheath unexpectedly combusted totally and are assigned to Class IV like pure PET. One explanation is that the PPS sheath inhibits the PET to drop. The resulting wicking-effect could lead to direct transport of the molten PET to the flame source, such acting as flame promoter, an effect which is known from inorganic flame retardants distributed homogenously in foams.[33] In consequence the PET combusts in the core. For this reason bicomponent fibers with PPS in the sheath are not suitable for fire protection as long as the core material is easily inflammable.

TABLE III
Results of Gravimetric Analysis After Chemical Treatment

	PPS/PET in KOH	PPS/PET in NaOH	PET/PPS in KOH	PET/PPS in NaOH
Weight before (mg)	752.3	752.8	762.8	762.5
Weight after (mg)	713.5	681.7	762.8	761.8
Reduction (%)	5.2	9.4	0.0	0.1

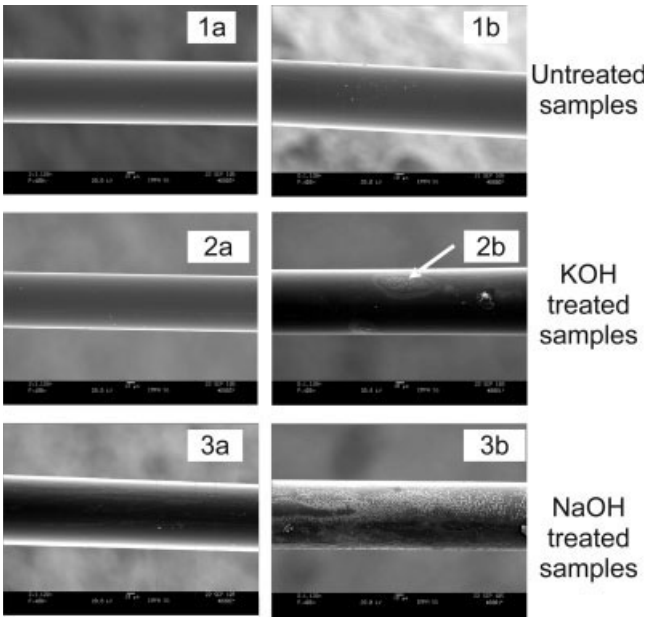

Figure 12 (1a) untreated PET/PPS fiber; (1b) untreated PPS/PET fiber; (2a) KOH-treated PET/PPS fiber; (2b) KOH-treated PPS/PET fiber; (3a) NaOH-treated PET/PPS fiber; (3b) NaOH-treated PPS/PET fiber.

Chemical resistance

The resistance of bicomponent fibers with a thin PPS sheath—PET/PPS (2/1)—and a thick PET sheath—

PPS/PET (1/2)—against two aqueous alkali solutions (40% (9.9*M*) KOH and 35% (12.1*M*) NaOH) was tested and afterwards measured gravimetrically and microscopically by SEM. The hydrolysis reaction starts at the fibers' peripheries, causing weight loss.[39] The weight loss is shown in Table III and the surface structures investigated by SEM in Figure 12(1a–3b).

Bicomponent fibers with PET in the sheath showed significant changes in weight and surface structure, as expected. Interestingly, the measured weight losses between 5.2% and 9.4% are relatively small in comparison with the observed weight losses during hydrolysis of other polyesters like poly(trimethylene terephthalate) (PTT)[25] and poly(butylene terephthalate) (PBT).[16] Kotek and Zeronian reported on weight losses larger than 15%, strongly depending on spinning speed and hydrolysis time.[16,25] The difference in weight loss between the NaOH and KOH can be explained by the higher concentration of the NaOH solution and, presumably, by the better mobility of the smaller Na^+-ions into the pores of the PET-sheath. Therefore the surface structure of the NaOH-treated fibers appeared more scale-like [Fig. 12(3b)] compared with the KOH-treated sample [Fig. 12(2b)].

Bicomponent filaments with PPS in the sheath did not show important changes in weight loss and no visible changes at the surface (Fig. 12). The small weight loss of 0.1% indicates that there might be a diffusion of alkali through the protective PPS-layer. Hence, a thin PPS sheath is sufficient to protect bicomponent fibers against the influence of strong alkali solutions for at least 16 h at room temperature.

CONCLUSION

Core-sheath bicomponent fibers consisting of the high-performance polymer PPS and PET were developed having well-defined counts with PPS both as core and sheath material. The effects of process conditions on the crystallinity and the mechanical properties were studied. The draw ratio, the core/sheath volume ratio and the composition of the bicomponent fibers were the main effective process variables. Both the crystallinity and the tensile strength of the bicomponent fibers increased with increasing draw ratio. It was found that the total crystallinity was higher for the PPS/PET system compared with that of the PET/PPS system. The core/sheath volume ratio was used in the PPS/PET system to switch between high or low crystallinity of the polymer components. Possible mechanisms of cavity formation were taken into consideration. Cavities at the PPS/PET interface occurred most likely due to fast cooling and different flow velocities.

Flammability was measured and classified. Contrary to expectation the bicomponent fibers with PPS both as sheath and core material worsened the flame retardancy in inhibiting the PET to drip, showing a wicking-effect. Hence, these bicomponent fibers are not suitable for use in fire protection. Study of chemical resistance showed that a thin PPS sheath is efficient to protect the PET-core against alkaline hydrolysis, thus imparting the functionality of chemical resistance to the bicomponent fiber.

We acknowledge B. Wüst for assistance during the melt spinning, Mr. Brück for information about PPS, and Ticona GmbH for supplying the PPS material.

References

1. Koch, P. A. Chemiefasern-Textilindustrie 1979, 81, 431.
2. Fourné, F. Synthetic Fibers Machines and Equipment, Manufacture, Properties; Carl Hanser Verlag: Munich, 1999.
3. El-Salmawy, A.; Kimura, Y. Text Res J 2001, 71, 145.
4. McCulloch, W. J.; Hagewood, J. Nonwovens World 2001, 10, 108.
5. Thönessen, F.; Dahringer, J. Chem Fibers Int 2003, 53, 422.
6. Baker, B. Int Fiber J 1998, 13, 26.
7. Watzl, A. Allgemeiner Vliesstoff Rep 1999, 4, 37.
8. Ziabicki, A. Fundamentals of Fibre Formation; Wiley: New York, 1976.
9. Chen, G. Y.; Cuculo, J. A.; Tucker, P. A. J Appl Polym Sci 1992, 44, 447.
10. Kiang, C. T.; Cuculo, J. A. J Appl Polym Sci 1992, 46, 67.
11. Kiang, C. T.; Cuculo, J. A. J Appl Polym Sci 1992, 46, 83.
12. Lin, C. Y.; Tucker, P. A.; Cuculo, J. A. J Appl Polym Sci 1992, 46, 531.
13. Kikutani, T.; Radhakrishnan, J.; Arikawa, S.; Takaku, A.; Okui, N.; Jin, X.; Niwa, F.; Kudo, Y. J Appl Polym Sci 1996, 62, 1913.
14. Cho, H. H.; Kim, K. H.; Kang, Y. A.; Ito, H.; Kikutani, T. J Appl Polym Sci 2000, 77, 2267.
15. Hada, Y.; Shikuma, H.; Ito, H.; Kikutani, T. J Macromol Sci Phys 2005, 44, 549.
16. Zeronian, S. H.; Inglesby, M. K.; Pan, N.; Lin, D.; Sun, G.; Soni, B.; Alger, K. W.; Gibbon, J. D. J Appl Polym Sci 1999, 71, 1163.
17. Shingankuli, V. L.; Jog, J. P.; Nadkarni, V. M. J Appl Polym Sci 1994, 51, 1463.
18. Nadkarni, V. M.; Shingankuli, V. L.; Jog, J. P. J Appl Polym Sci 1992, 46, 339.
19. Jog, J. P.; Shingankuli, V. L.; Nadkarni, V. M. Polymer 1993, 34, 1966.
20. Ravindranath, K.; Jog, J. P. J Appl Polym Sci 1993, 49, 1395.
21. Shingankuli, V. L.; Jog, J. P.; Nadkarni, V. M. J Appl Polym Sci 1988, 36, 335.
22. Carr, P. L.; Ward, I. M. Polymer 1987, 28, 2070.
23. Radhakrishnan, J.; Kikutani, T.; Okui, N. Text Res J 1997, 67, 684.
24. Nelson, M. I. Combust Theor Model 2001, 5, 59.
25. Kotek, R.; Jung, D. W.; Kim, J. H.; Smith, B.; Guzman, P.; Schmidt, B. J Appl Polym Sci 2004, 92, 1724.
26. Dugan, J.; Srinivasan, R. Technical Textile Technology, December 2005, p 64.
27. Hufenus, R. Ph.D. Thesis, ETH No 16177, Zurich, 2005.
28. ISO 2060; International Organization for Standardization: Geneva, Switzerland, 1993.

29. ISO 2062; International Organization for Standardization: Geneva, Switzerland, 1994.
30. DIN 53765; Testing of plastics and elastomers; German Institute for Standardization: Berlin, Germany, 1994.
31. Wunderlich, B. Thermal Analysis; Academic Press: San Diego, 1990.
32. Huo, P.; Cebe, P. Colloid Polym Sci 1992, 270, 840.
33. Troitzsch, J. International Plastics Flammability Handbook; Hanser: Munich, 1990.
34. http://www.kern-gmbh.de/.10 November, 2006.
35. Ku, T. H.; Lin, C. A. Text Res J 2005, 75, 681.
36. Heuvel, H. M.; Huisman, R. J Appl Polym Sci 1978, 22, 2229.
37. Shingankuli, V. L.; Jog, J. P.; Nadkarni, V. M. J Appl Polym Sci 1988, 36, 335.
38. El-Salmawy, A.; Miyamoto, M.; Kimura, Y. Text Res J 2000, 70, 1011.
39. Collins, M. J.; Zeronian, S. H.; Semmelmeyer, M. J Appl Polym Sci 1991, 42, 2149.